# INCEPTION OF STALL IN A CENTRIFUGAL IMPELLER

by

K.MURUGESAN AND S.RAMAMURTHY
(Scientists, Propulsion Division, National Aerospace Laboratories
Bangalore-560 037, India)

## SUMMARY

Measurements at outlet of a centrifugal impeller show spatial and temporal variations of flow velocity. There is pitch-wise symmetry and time-wise repetitiveness with impeller rotation at large flow coefficients. This flow structure undergoes changes as the flow coefficient is reduced from a large value, by throttling, towards stall. A newly evolved parameter characterises these changes and helps to identify regions of instability and rotating stall. The correlation between this instability parameter and flow coefficient is very clear and quite good. The magnitude of this parameter value could be used to identify the inception of stall in centrifugal impellers so as to activate control mechanism.

## Nomenclature

C absolute velocity(m/s)
$C_p$ specific heat at constant pressure (kcal/kg K)
D diameter (m)
m mass flow rate (kg/s)
P pressure ($N/m^2$)
P pressure surface
PR total-total pressure ratio
S suction surface
T temperature (K)
U peripheral speed (m/s)
$\phi$ flow coefficient
$\Psi$ pressure rise coefficient
$\Delta$ differential
$\gamma$ ratio of specific heats
$\rho$ density ($kg/m^3$)

## Subscripts

av average
min minimum
max maximum
o stagnation condition
r radial
t tangential
1 impeller inlet
2 impeller outlet



## 1. INTRODUCTION

Flow instabilities such as rotating stall and surge have large influence on the compressor characteristics. These contribute to vibratory excitation and performance deterioration. It is important to detect and avoid or control these. Many authors[1,2,3,4,5,6,7] have carried out experimental investigations to characterise rotating stall in terms of propagating speed and number of stall cells. There has however been few attempts for early detection or investigation of the phenomenon leading to rotating stall. Very recently Day[8] has suggested some means for active control of surge and stall. Rotating stall is characterised as periodic breakdown of energy transfer from the rotor to the flow within a portion of the impeller channel, at any given time[9]. The flow at outlet of the impeller, even in stall free operation, is unsteady due

to the vortex type of disturbance created within the blade channels of the rotor[10,11,12]. Such flows with discrete vortices are generally confined to small regions and co-exist with a steady jet flow within each bladed channel of the rotor. These are periodic and are related to rotational speed of the impeller[13,14]. The pitchwise symmetry and time-wise periodicity or repetition of flow for every revolution are essential for stable operation of the impeller.

## 2. EXPERIMENTAL SET-UP

Stall, in particular, incipience of it, can be effectively analysed by a study of flow property details collected at impeller outlet using hot-wire anemometry. Measurements were carried out at outlet of a centrifugal impeller in a closed circuit test facility. The schematic view of the test facility is shown in Figure-1.

The geometrical details of the test compressor are given below

| | |
|---|---|
| Impeller tip dia. | 300 mm |
| Impeller tip width | 7 mm |
| Impeller blades | 19 |
| Backsweep angle | 30 deg |
| Diffuser inlet dia. | 315 mm |
| Diffuser exit dia. | 452 mm |
| Diffuser blades | 17 |

The impeller was rotated at a constant speed of 7000 rpm by a DC motor. Thyristor control with feed back for the DC motor ensured maintenance of the speed to an accuracy of 0.1%. The compressor and DC motor were connected together through a stepup gear box. An electronic torquemeter coupled in between the gearbox and the compressor was used to measure compressor speed and input power. A gate valve provided in the closed circuit was used to vary the massflow rate through the compressor. A heat exchanger in the closed circuit was used to ensure steady inlet

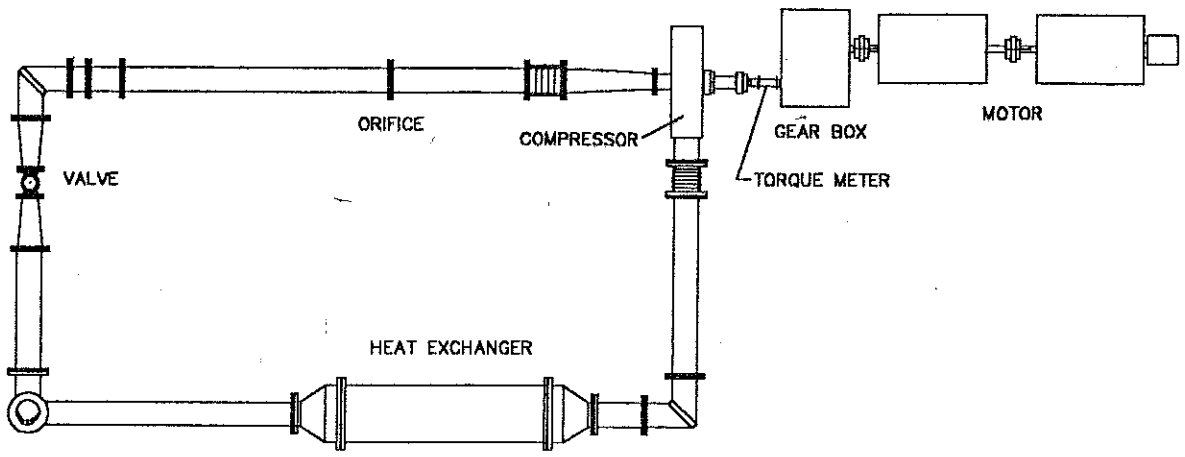


Fig. 1 Schematic Layout of Test Facility

flow conditions.

## 3. INSTRUMENTATION

The test facility was instrumented for detailed flow measurements at impeller outlet. A hot-wire sensor shown in Figure-2 was placed at a nearby position radially outward from the impeller tip. The sensor had two tungsten wires of 5 micron diameter placed perpendicular to each other. The sensor was oriented to measure radial and tangential components of absolute velocity in dynamic mode. The measurements were taken continuously for nearly three revolutions at mid section between hub and shroud side wall of the impeller. Two linearisers were used in conjunction with the hot-wire anemometer circuit. Calibration was carried out separately in a steady uniform flow before and after the experiments for the range of velocities. The measurement accuracy of velocity was +/- 5%. The hot-wire traces were captured through a computer controlled dual beam signal analyzer and recorded through its memory onto magnetic disks. The instrumentation layout and measurement points are shown in Figure-3. Once per revolution pulse generated from an eddy current probe, due to a small projection in the shaft, was used to trigger simultaneously both the hot wire traces. The hot-wire signals were recorded for a duration of 25 milliseconds which correspond to more than 2 revolutions of the impeller. Over this period the signal was digitised into 2048 data recordings. This provided a frequency response of 20kHz., while the blade passing frequency was 2.2kHz. Fifty such recordings one after the other in a phase-locked manner were summed up to get an ensemble average of the signal. In addition, the instantaneous trace as a raw signals of both hot-wires were also collected at the end of the ensemble averaging process.

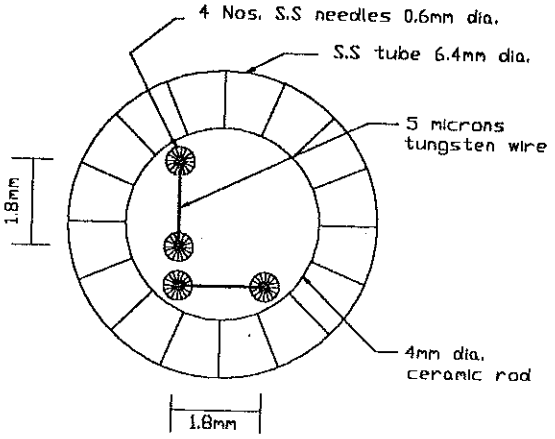

TOP VIEW OF HOT-WIRE SENSOR

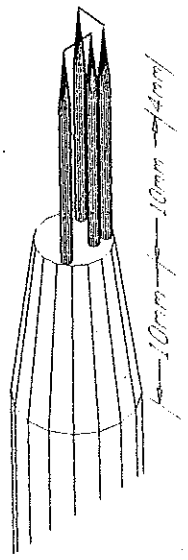

Fig. 2 Hot-wire sensor

## 4. EXPERIMENTAL RESULTS

Experiments were carried out at different flow coefficients with close

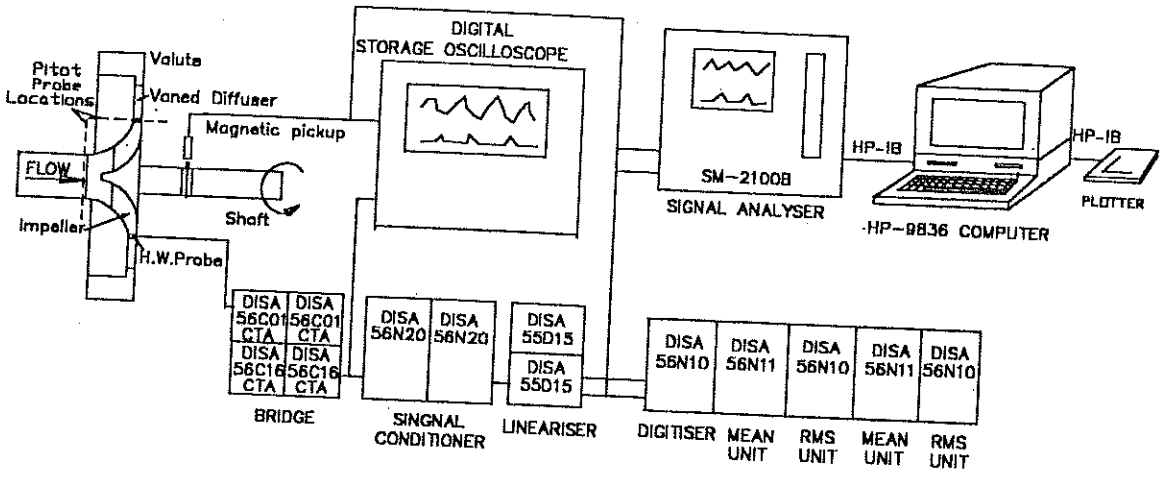


Fig. 3 Layout of Hot-Wire Anemometry System

intervals including the stalled region. Apart from hot-wire anemometry, global parameters were also collected using pitot tube pressure measurements. From the global parameters flow coefficient,($\phi$) and pressure rise coefficient,($\Psi$) at different operating points of the compressor were estimated using the following formulae.

$$\phi = \frac{4\ m}{\rho_{o1}\ \pi\ D_2^2\ U_2} \quad \ldots\ldots(1)$$

$$\psi = \frac{2\ C_p\ T_{o1}\ (PR^{(\gamma-1)/\gamma} - 1)}{U_2^2} \quad (2)$$

The pressure rise coefficient versus flow coefficient characteristic of the compressor thus obtained is shown in Figure-4.

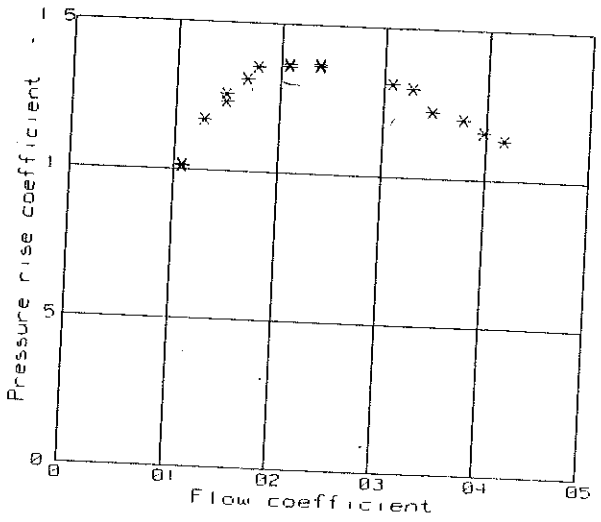


Fig. 4 Impeller Characteristic

At each flow coefficient, both radial($C_r$) and tangential($C_t$) components of absolute velocity were measured using the two hot-wires of the anemometry probe. For each of the velocity component, an ensemble-averaged signal as well as one instantaneous raw signal were collected within a duration of 25 ms. Such hot-wire measurements collected at six flow coefficients with compressor speed of 7000 RPM are analysed and discussed

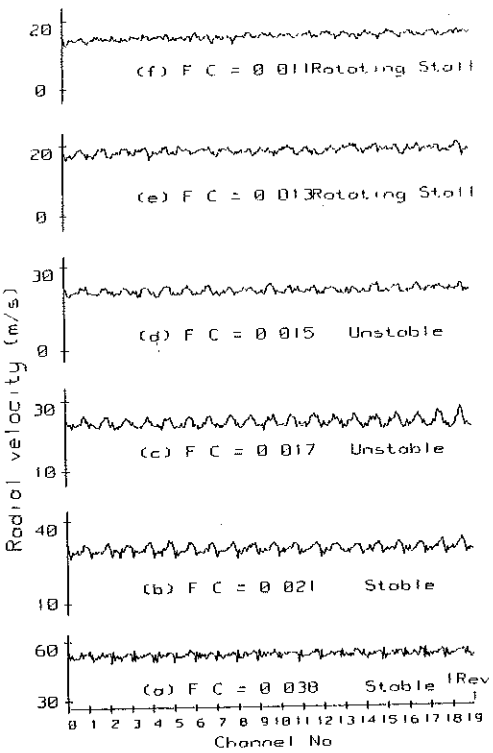


Fig 5 Radial velocity
(Ensemble averaged)

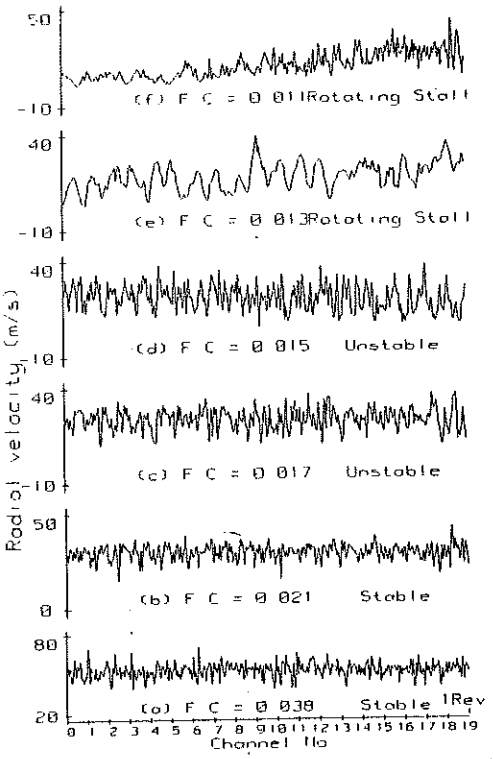


Fig 6 Radial velocity
(Raw signal)

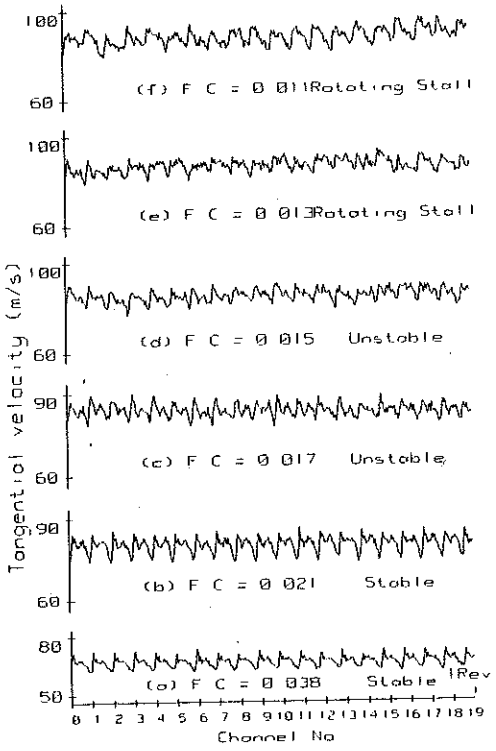


Fig 7 Tangential velocity
(Ensemble averaged)

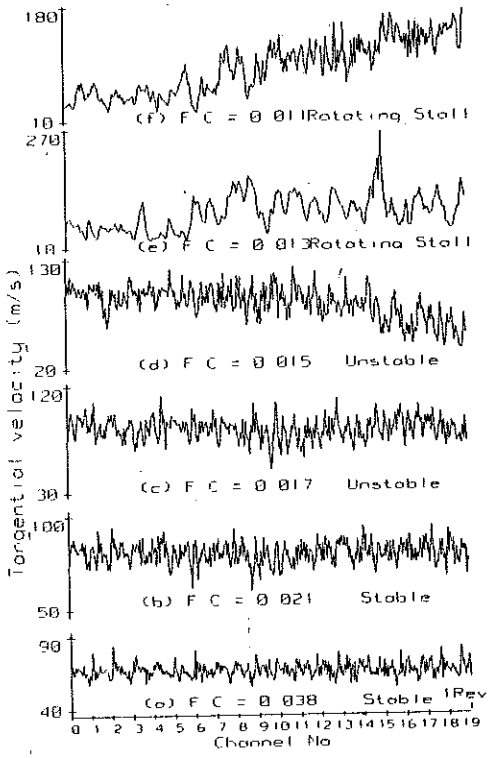


Fig 8 Tangential velocity
(Raw signal)

hereunder. The trace signals are given in Figures-5, 6, 7 and 8. The radial component of absolute velocity $C_r$, after ensemble averaging is given in Figure-5, while the raw signal of $C_r$ is given by the side in Figure-6. Similarly, the tangential component of velocity $C_t$, after ensemble averaging, is given in Figure-7 while the raw signal of $C_t$ is given in Figure 8. Signal traces for six flow coefficients are given in each figure with subscripts a to f. These flow coefficients are denoted as FC and are respectively ' 0.038, 0.021, 0.017, 0.015, 0.013, and 0.011. For the sake of clarity, different scales are used along the ordinate in different figures.

The trace signals of $C_r$ and $C_t$ are for one revolution of the impeller, comprising of flow in 19 bladed channels. Figures 5a & 5b, 6a & 6b, 7a & 7b and 8a & 8b indicate that at large flow coefficients the flow in individual channels are symmetric and nearly identical with each other. There is also general resemblence between the raw signal and the ensemble averaged signal. This symmetry in pitch-wise direction and similarity between ensemble averaged and raw signals are maintained until the flow coefficient is reduced to 0.021 from 0.043. Thereafter, the flow structure across a blade pitch changes with flow coefficient, which is observed at lower flow coefficients. Some distinct observations can be made by looking at the ensemble averaged signals in Figures 5 and 7. It may be noted that the differing scales are marked respectively in each figure. As the flow coefficient is reduced, the through-flow or radial component of velocity, $C_r$ reduces, while the tangential component of velocity, $C_t$ increases. This is consequent to increase in pressure rise coeficient, when the flow coefficient decreases as in Figure-4. However, at very low flow coefficients, near stall, there is no further increase in the value of tangential component of velocity $C_t$ as in Figure 7e and 7f. Upon ensemble averaging, if at all, there are less variations of velocity within a blade channel at lower flow coefficients. By and large the pitch-wise symmetry is seen to be retained in the ensemble averaged velocities. On the other hand, the flow structure as seen from the raw signal traces of velocity components in Figures 6 and 8 are vastly different. Flow variations across some blade pitch in the raw signal are much more at lower flow coefficients and differ a lot between any two blade pitch. Variations in flow velocity within a blade pitch are due to the vortex type of disturbances inside the rotor as discussed in the introductory paragraph. These variations are particularly predominant in the tangential velocity component as in Figures-8c,d,e & f. Thus , as the flow coefficient is reduced, the instantaneous velocity variations, within individual channels of the raw signal, are getting amplified with increasing difference between channels. This is contrasted by the reduction in magnitude of variation in velocity for the ensemble averaged signal. The loss of increase in magnitude of

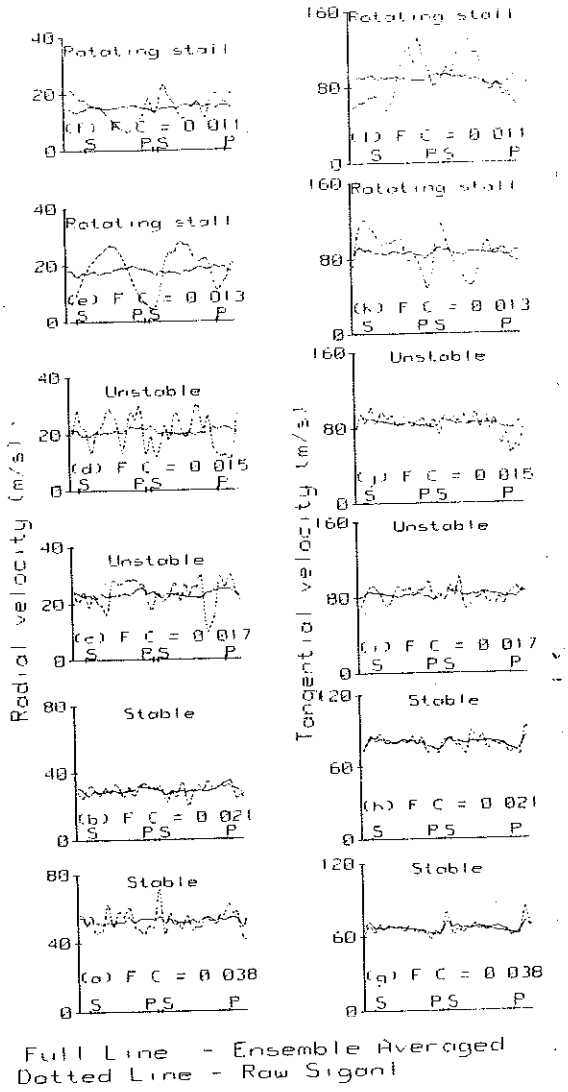


Fig. 9 Flow Structure

variation in ensemble averaged signal, at low flow coefficients, is due to the fact that the flow structure in an individual channel is not repetitive and is getting altered from one revolution to another. This shows that once per revolution time-wise periodicity or coherence is slowly breaking up and the flow is getting de-stabilised from a repetitive flow. An important point of observation is that such de-stabilisation of flow is ahead of the onset of stall. In fact, at flow coefficients, between 0.021 and 0.017, there is no sudden drop in tangential component in any packet of channels.

A more closer comparison of ensemble averaged velocity and the instantaneous velocity variations within a channel could be made. These are depicted for two channels in Figure-9, for both the radial component $C_r$ and the tangential component $C_t$. These are derived by transforming the timewise variation of velocity measurements to spatial variation. Through the transformation the corresponding channel suction and pressure surface trailing edges were identified and are marked as S and P in Figures-9a to 9l. From a study of velocity trace as a raw signal contrasted with the corresponding ensemble averaged signal, it is seen that the operating range can be divided into two regions, one with good stability and an other region, where the flow is getting de-stabilised. This region of instability is characterised by the fact that in any individual channel the instantaneous flow structure is very much different from the corresponding ensemble averaged flow, although none of the channels is stalled as such. At low flow coefficients (even ahead of stall), there are large variations in instantaneous velocity within a channel revealed by the raw signal trace. This is contrasted by the reduction in variations of velocity for the ensemble averaged signal trace. These are clearly seen in Figures-9c,d,e,f and 9i,j,k,l.

On the contrary, in a stable region of operation, there is very close resemblence and coherence between the instantaneous flow structure and the ensemble averaged one. The instability as analysed above is much more apparent in terms of magnitude in the tangential component $C_t$. It is at the lower flow coefficients of less than 0.017, the tangential component of velocity is seen to deviate more and more from a repetitive once per revolution flow.

## 5. DISCUSSIONS

The foregoing analysis of experimental results suggest that at low flow coefficients, with an increase in pressure rise coefficient, there are bursts of large differential tangential velocities within one channel which are not in resonance with impeller rotation. These tend to de-stabilise the process of energy transfer and flow structure in the impeller. It can easily be reasoned out why the tangential component of velocity is the predominant factor for stability. The loading or energy transfer to the fluid is a product of impeller rotational speed and the change in tangential velocity from inlet to outlet. In this case, the inlet tangential velocity was zero and experiments had been carried out at a constant rotor speed. The estimate of the term $(\Delta C_t) = C_{t,max} - C_{t,min}$ within one blade passage, would give the variation of energy transfer. Whenever this is not in resonance with impeller rotation the flow is bound to be de-stabilised. The ensemble averaged signal would retain only the repetitive or coherant component. Thus the factor, which directly influences the instability of the flow structure, would be the difference of this term $\Delta c_t$, as in the raw signal and the ensemble averaged one. Such a factor would quantify the analysis, made in the earlier paragraph, of the behaviour of velocity components with varying flow coefficient. In order to make the term non-dimensional and define a parameter to characterise instability, the maximum to minimum differential of tangential velocity in one channel was divided by the average radial component of velocity within that channel. This was found to reduce the scatter in the experimental data and correlate the phenomenon of instability more clearly. Thus, an ***instability parameter, IP***, is defined as

$$IP = \frac{(\Delta C_t)_{raw}}{(C_{r,av})_{raw}} - \frac{(\Delta C_t)_{ensemble}}{(C_{r,av})_{ensemble}}$$

Where $(\Delta C_t) = C_{t,max} - C_{t,min}$

Values of this instability parameter for each of the 19 channels in one revolution were evaluated for nine flow coefficients. These are plotted against respective flow coefficients in Figure-10. The average of all 19 channels, at a given flow coefficient is also marked as a correlating line. This correlation is seen to be very good. In the evaluation of this parameter, flow properties in a particular channel, whether as raw signal or ensemble averaged one were used. Hence the value of the instability parameter, indicates the amount of de-

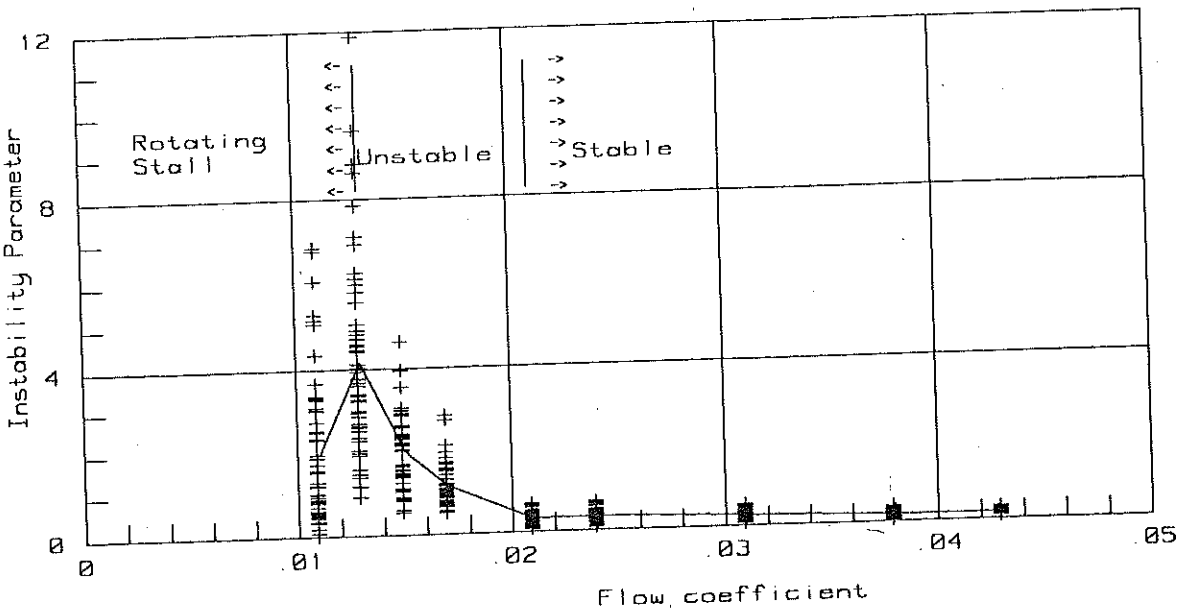


Fig. 10 Correlation for Flow Instability

stabilisation that is contributed by the flow in that channel. In Figure-10, it is seen that this number is very nearly zero for all channels in the stable region of large flow coefficients higher than 0.021. At lower flow coefficients, the value increases sharply. Individual values, of instability parameter, suddenly increase to 3,5 and even 10 and above as the flow coefficient reduces. The average of instability parameter value of all channels of one impeller rotation jumps, from near zero, to 1 at flow coefficient of 0.017 and subsequently increases to 2 at the close by flow coefficient of 0.015. This clearly demarcates the region of instability from that of stable operation. The two regions, viz. stable and unstable are marked in the Figure-10 by a demarcating line at the flow coefficient of 0.021, when the instability parameter sharply rises in its value from very nearly zero. What is more interesting is that there is a large scatter in the value of instability parameter for different channels. Every individual channel flow is unrelated to other channels and not repetitive with impeller rotation. This essentially characterises instability. Individual channel flow is getting out of control from impeller rotation. At a flow coefficient of 0.013, the bursts of instability are vigorous and the individual channel instability parameters reach values as high as 10 and above in Figure-10. They are also numerous as seen from the larger number of channels having higher values. The initiation and timing of the de-stabilising disturbances in some of the channels are so random that these tend to spill over and start affecting the

neighbouring channels. Such influencing of neighboring channel flow, with a large scatter in instability bursts, pushes the flow to coagulate into pockets. Now these pockets of instability could be moving with some correspondence to impeller rotation so that the overall flow is once again some-what repetitive. Thus the impeller is pushed into a flow region of rotating stall, which could be comparatively stable, with variations in energy transfer arranged in a fashion, periodic with impeller rotation. Operation of the compressor with clearly identifiable rotating stall was indeed located at this flow coefficient of 0.011 and is marked in Figure-10.

## 7. CONCLUSIONS

The outlet flow from a centrifugal impeller has been analysed at various flow coefficients, using a newly evolved instability parameter, IP. There is a good correlation between this parameter and the flow coefficient. The characteristic clearly demarcates regions of stable operation, instability and rotating stall. The demarcation of instability is through identifiable bursts of velocity differentials within a blade channel which are not in repetitive coherence with impeller rotation. Since this phenomenon occurs well ahead of stalling of the impeller flow, detection of this through the instability parameter will be advantageous. Evaluation of this parameter, from measurements, only at that one point of operation would indicate the range available before stall. The timing for corrective action as well as mode of action are available ahead of actual stall.

## 6. ACKNOWLEDGEMENT

Useful discussions were held with Professor S.Soundaranayagam, Scientist Emeritus, NAL during the initial preparation of this manuscript. The authors wish to thank Mr.S.Sankara Narayanan for the collection of experimental data and Mr.R.Rajendran for the technical assistance during experiments. Some of the hardware for this work was funded by AR & DB earlier.

## 7. REFERENCES

1. Van Den Braembussche.R.A.,& Roustan.M., "Rotating non-uniform flow in radial compressors",Agard conference, Proc. No. 282,Centrifugal Compressor Flow Phenomenae and Performance.

2. Kubo.T.&Murata.S.,"Unsteady flow phenomena in cetrifugal fans",Ist report, Rotating Flow Patterns in an Inlet Duct,Bull.JSME,Vol.19 No. 135,Sep.1976,PP:1039-1046.

3. Kinoshita.Y. & Senoo.Y., "Rotating stall induced in vaneless diffusers of very low specific speed centrifugal blowers", ASME Paper 84-GT-203,1984.

4. Frigne.P. & Van Den Braembussche.R.,"A theoretical model for rotating stall in vaneless diffuser of a centrifugal compressor", ASME Paper 84 - GT - 204, 1984.

5. Otugen.M.V. & Hwang.B.C., "The effects of diffuser geometry on rotating stall behaviour", ASME Paper 88-GT-153,1988.

6. Breugelmans,F.A.E., "Axial flow compressor rotating stall", VKI L.S -1992-02, Belgium.

7. Breugelmans,F.A.E.,& Blanco,E.M., "3-D Flow measurements in the relative frame of reference during rotating stall",X ISABE, Nottingham, U.K.,Sept,1991, PP-944-951.

8. Day,I.J.,"Review of stall, Surge and active control in axial compressors",XI ISABE Tokyo,Japan,Sept.,1993, PP: 97-105.

9. Camber.N. & Rautenberg.M., A distinction between different types of stall in a centrifugal compressor stage", Jl. Engg. Gas Turbine and Power,Jan. 1986 Vol.108/83,PP: 83-89.

10. Ramamurthy.S.&Murugesan.K., "Flow behaviour in centrifugal impellers",Xth ISABE 1991.

11. Ramamurthy.S.&Murugesan.K., "Correlations for flow property variation at outlet of a centrifugal impeller", XI-ISABE,1993.

12. Krain,H.,"Experimental and theoretical analysis of centrifugal impeller flow" Int. conf. on Turbomachinery,Proc. of the I. Mech. E., C270/87, PP: 199-210, Sept. 1987.

13. Ramamurthy,S.&Murugesan,K., "Spectral fluctuations in centrifugal impeller outlet flows",Air Breathing Engines and Aerospace Propulsion, Proceedings of NCABE-94, PP:365-380.

14. Sankaranarayanan,S., Murugesan,K. & Sane,S.K., "Experimental detection of unsteady flow at the entry to vaneless diffuser of a centrifugal compressor", Air Breathing Engines and Aerospace Propulsion, Proc. of NCABE-94,Poster Session.